Three-dimensional, time-resolved velocity and density measurements of the stratified shear flow in an inclined duct

Adrien Lefauve, Jamie L. Partridge, Stuart B. Dalziel and P. F. Linden

Department of Applied Mathematics and Theoretical Physics
University of Cambridge, Wilberforce Road, Cambridge, CB3 0WA, UK
lefauve@damtp.cam.ac.uk

Abstract

Laboratory experiments on the stratified shear flow in an inclined duct are reported. Stratified turbulence is observed in this two-layer exchange flow, whose dissipation is controlled by the duct inclination and compares in intensity with that observed in geophysical contexts. A setup enabling three-dimensional (3D) simultaneous Particle Image Velocimetry (PIV) and Laser-Induced Fluorescence (LIF) is presented, and applied to the visualisation of Holmboe waves. Such capabilities are believed to be key to advance our understanding of the dynamics and mixing of stratified turbulence in the near future.

1 The inclined duct experiment: introduction and motivation

Between large-scale, geostrophic turbulence and small-scale, isotropic turbulence lies a range of scales strongly affected by buoyancy. This is the realm of stratified turbulence, characterized by high Reynolds number (Re), low horizontal Froude number (Fr_h) but high buoyancy Reynolds number ($Re_b \equiv Re\, Fr_h^2$, sometimes referred to as turbulent intensity), which exhibits complex dynamics and mixing properties (Waite, 2014). Although in typical geophysical settings the turbulent intensity can be extremely large $Re_b = O(10^5 - 10^7)$, Bartello and Tobias (2013) argued that $Re_b > O(10)$ was sufficiently high to investigate this regime. However, sustaining high-Re and high-Re_b to investigate the stratified turbulence regime proves challenging both experimentally and numerically.

The experimental setup sketched in figure 1 consists of a long duct of square cross-section connecting two reservoirs of salt solutions at slightly different densities ρ and $\rho + \Delta\rho$. When the duct is opened, a two-layer counter flow develops and becomes established for

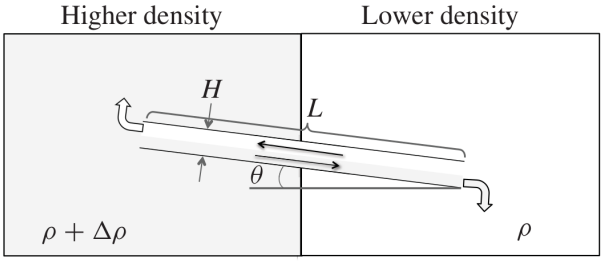

Figure 1: Schematic of the inclined duct experiment. Adapted from Meyer and Linden (2014)

extended periods of time, until the higher-density solution reaches the level of the duct in the lower-density reservoir, and vice versa. A flexible barrier between the two reservoirs allows the duct to be inclined at an angle θ from the horizontal. Both reservoirs have a free surface such that to a very good approximation, the flow through the duct has zero net volume flux.

Similar buoyancy-driven exchange flow experiments in rectangular ducts were first introduced by Macagno and Rouse (1961) and Kiel (1991). Both studies highlighted the diversity of flow regimes observed. As the flow speed is increased by the density difference $\Delta\rho$ or the angle θ, interfacial waves can develop on the initially undisturbed, sharp interface between the two laminar, counter-flowing layers. Further increase in the flow speed can lead to the onset of turbulence in the interfacial region, and eventually to increasing turbulence and mixing intensities, until the turbulent mixed layer almost completely fills the duct. While Macagno and Rouse (1961) mapped the different flow regimes and estimated the interfacial friction coefficient, Kiel (1991) performed mass transport measurements and proposed a Bernoulli-type model to predict the exchange flow velocity as well as an empirical entrainment model.

More recently, Meyer and Linden (2014) introduced the setup shown in figure 1 ($H = 10$ cm, $L = 300$ cm and 150 cm) and mapped four qualitatively distinct regimes in the $(\Delta\rho/\rho, \theta)$ plane, based on shadowgraph visualisations. Figure 2 gives examples of such regimes using shadowgraph images, together with subsequent more quantitative density and vorticity measurements, all made in a smaller apparatus ($H = 4.5$ cm, $L = 135$ cm) which will be used throughout the rest of the paper. The laminar state with an undisturbed interface and no wave activity ("L" state) is omitted, and increasing $\Delta\rho$ or θ successively leads to Holmboe waves at the interface ("H" state), intermittent turbulence and mixing ("I" state), and fully-developped turbulence in a thick mixed layer ("T" state). Meyer and Linden (2014) argue that the flow is hydraulically controlled at both ends of

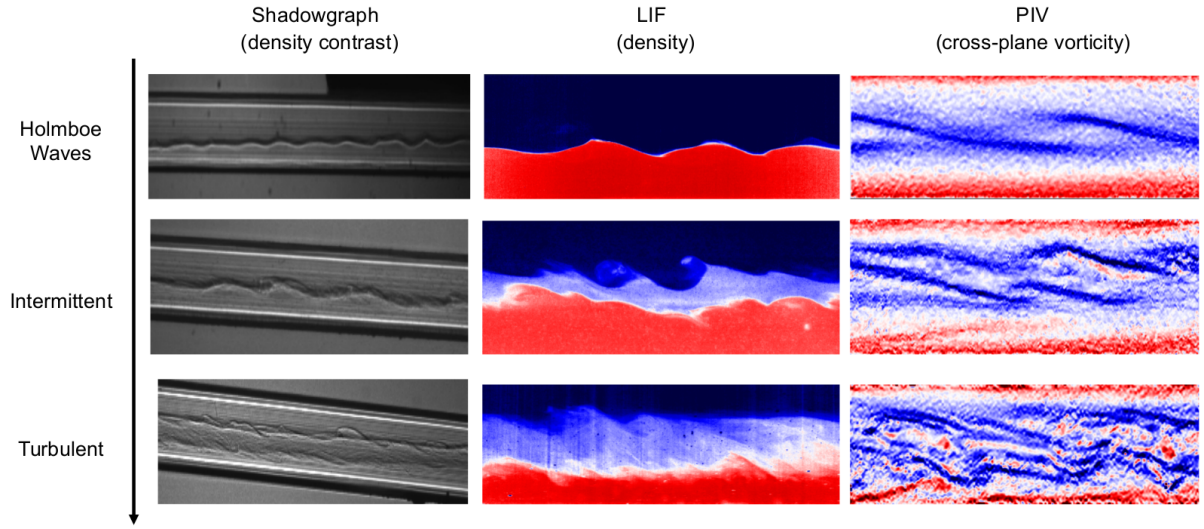

Figure 2: Flow regimes examples visualised over a horizontal window of ~ 20 cm (not simultaneous: each image corresponds to a different experiment). Here Re is varied between $\approx 2000 - 4000$ and $\theta \approx 0 - 5°$. Shadowgraphy comes from the convergence and divergence of parallel light traversing the flow because of variations in refractive index. Laser Induced Fluorescence (LIF) and Particle Image Velocimetry (PIV) are briefly explained in §2.

the ducts, due to the sharp change in cross-section geometry, giving an upper bound on the flow velocity of order $U \sim \sqrt{g'H}$ where $g' = \Delta\rho/\rho$. This is supported by mass flux measurements, from which volume fluxes can be inferred when little mixing occurs, suggesting layer-averaged velocities $U \approx 0.3\sqrt{g'H}$ when $\theta \approx 0$ (due to viscous friction) and a plateau at $U \approx 0.5\sqrt{g'H}$ for $1° \lesssim \theta \lesssim 4°$ in broad agreement with frictional

hydraulic theory. They further argue that the forcing from the hydrostatic pressure in each reservoir is sufficient to account for such velocities. Therefore, the additional kinetic energy gained by the flow as a result of the duct inclination θ must be dissipated turbulently, yielding a scaling for the turbulent transition which compares favourably with their data. Importantly, Meyer and Linden (2014) recognise the suitability of this experiment to investigate the energetic stratified turbulent regime. The kinetic energy dissipation in the duct ϵ is indeed controlled by the duct inclination θ, and rewriting Re_b as a ratio of dissipation to buoyancy frequency $Re_b = \epsilon/(\nu N^2)$, we can estimate

$$Re_b = \frac{\frac{\text{dissipation}}{\text{transit time}}}{\nu N^2} \sim \frac{\frac{g' L \sin\theta}{L/\sqrt{g'H}}}{\nu g'/H} \sim \frac{\sqrt{g'H}H}{\nu} \sin\theta \sim Re \sin\theta. \tag{1}$$

Given that $Re = O(10^3 - 10^4)$ is typically achievable in the current setup, this scaling suggests that high values of $Re_b = O(10^2 - 10^3)$ can be sustained for several minutes. Unlike other experiments in which turbulent mixing is achieved by an external mechanical input of kinetic energy, here turbulent mixing takes place internally within the flow and is driven by a constant gravitational forcing, making it particularly appealing for the study of geophysically-relevant stratified turbulence.

In this paper, we will present an experimental setup capable of 3D simultaneous measurements of the density and velocity fields. We shall first describe the setup in §2, before using it to visualise simple Holmboe waves in §3. We offer a brief summary as well as directions for future work in §4.

2 Experimental setup: 3D, time-resolved PIV and LIF

The setup is composed of the inclined square duct (length $L = 135$ cm, height and width $H = 4.5$ cm) connecting two reservoirs, one containing a dense solution sodium nitrate ($NaNO_3$) and the other a lighter solution of sodium chloride (NaCl) with carefully matched refractive indices (figure 3). A Litron laser emitting 532 nm, 100 mJ pulses at a frequency of 25 Hz is combined to traversing optics, which produces a thin ($\approx 1-2$ mm) light sheet oscillating back and forth in the spanwise (y) direction at speed 22 mm.s^{-1}. This system illuminates thin (x, z) planes in the flow in a window of ≈ 17 cm extent in x and scans this plane in y, in order to perform measurements in a 3D volume.

Two flow visualisation techniques are used simultaneously: stereo Particle Image Velocimetry (PIV) and Laser Induced Fluorescence (LIF), see figure 3a. PIV relies on tiny (≈ 20 μm) polyamide reflective particles being seeded in the flow and imaged in a (x, z) plane by two cameras (B and C) looking from different angles. LIF relies on marking the $NaNO_3$ solution with a fluorescent dye (rhodamine 6G). The dye has roughly the same diffusivity as $NaNO_3$, hence its concentration can be used to trace the concentration of $NaNO_3$, and hence the density. The light intensity emitted by the dye is imaged by camera A, from which the local dye concentration is deduced, which in turn allows the determination of the local density. While the particles emit the laser light at the original wavelength, the dye emits it at a slightly different wavelength, allowing to separate the PIV and LIF signals by ad hoc filters. Using 4 MPixel monochrome AVT Bonito cameras, 3D volumes of velocity and density fields at x, y, z resolutions of $\approx 200 \times 25 \times 60$ and $\approx 1500 \times 25 \times 450$ respectively, are achieved in a scan of duration 2 s (figure 3b). This 3D data is quasi-instantaneous in the sense that each of the 25 $y-$plane is shifted in time with

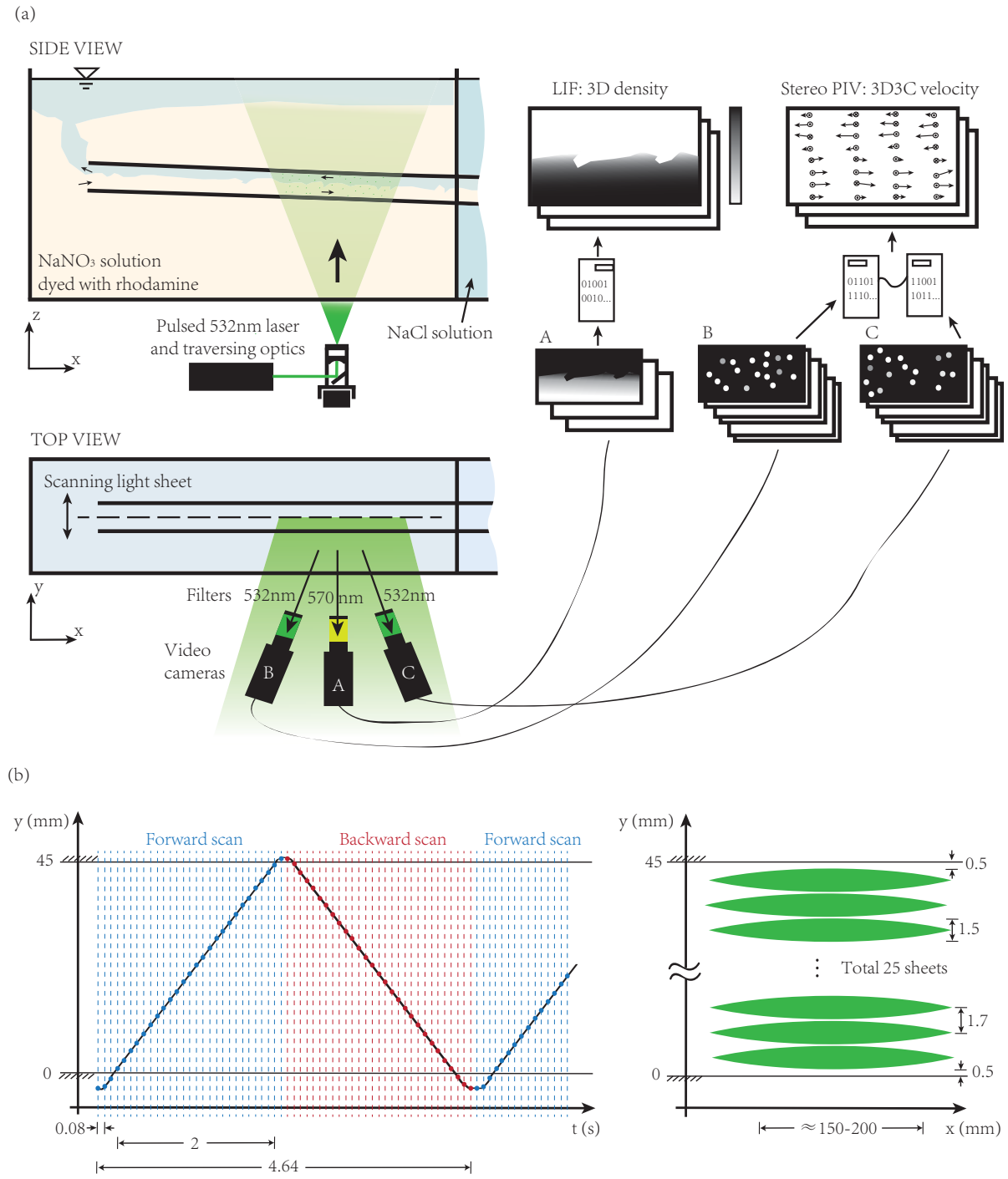

Figure 3: Schematic of (a) the 3D PIV and LIF setup, (b) the scanning light sheet settings.

respect to the previous one by 0.08 s. The data is also time-resolved, and with current memory capabilities, it is possible to record ≈ 400 such 3D volumes (200 in a forward scan, 200 in a backward scan), during an experiment of duration ≈ 15 min.

3 Application: visualisation of 3D Holmboe waves

The setup described in §2 is now applied to a flow in the Holmboe wave regime ($\Delta\rho/\rho = 1 \times 10^{-3}, \theta = 5°$), which has a characteristic velocity $\sqrt{g'H} = 21$ mm.s^{-1} and $Re =$

$\sqrt{g'H}H/\nu = 945$. Figure 4 shows quasi-instantaneous visualisations of such a flow: figure 4a is a perspective view combining the mid-density isosurface and 2D streamlines in the mid-plane $y = H/2 = 22.5$ mm, while figures 4b-c are 2D slices combining the density field and streamlines in $y = 22.5$ and 28 mm. Figure 5 is composed of the same data as figure 4a, on which the local cross-plane vorticity field is superimposed.

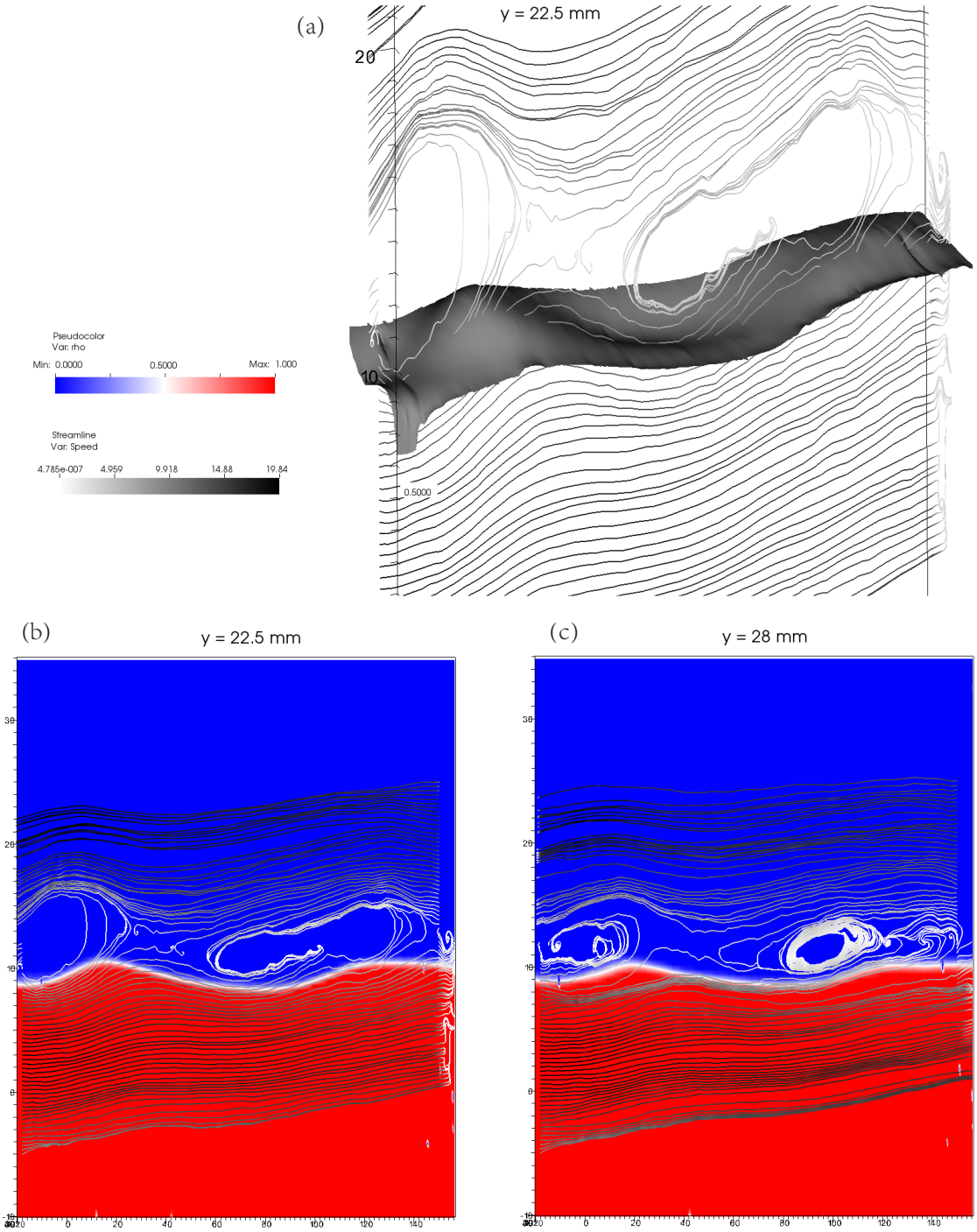

Figure 4: (a) Mid-density isosurface (grey with shadows) with 2D streamlines coloured according to local velocity magnitude (see legend in mm.s^{-1}) in the mid-plane $y = 22.5$mm. (b) and (c) (x,z) slices of false colour density field (see legend) and streamlines as in (a), in mid-plane and $y = 28$mm plane respectively. The z axis is stretched by a factor of 10 in (a) and 5 in (b),(c).

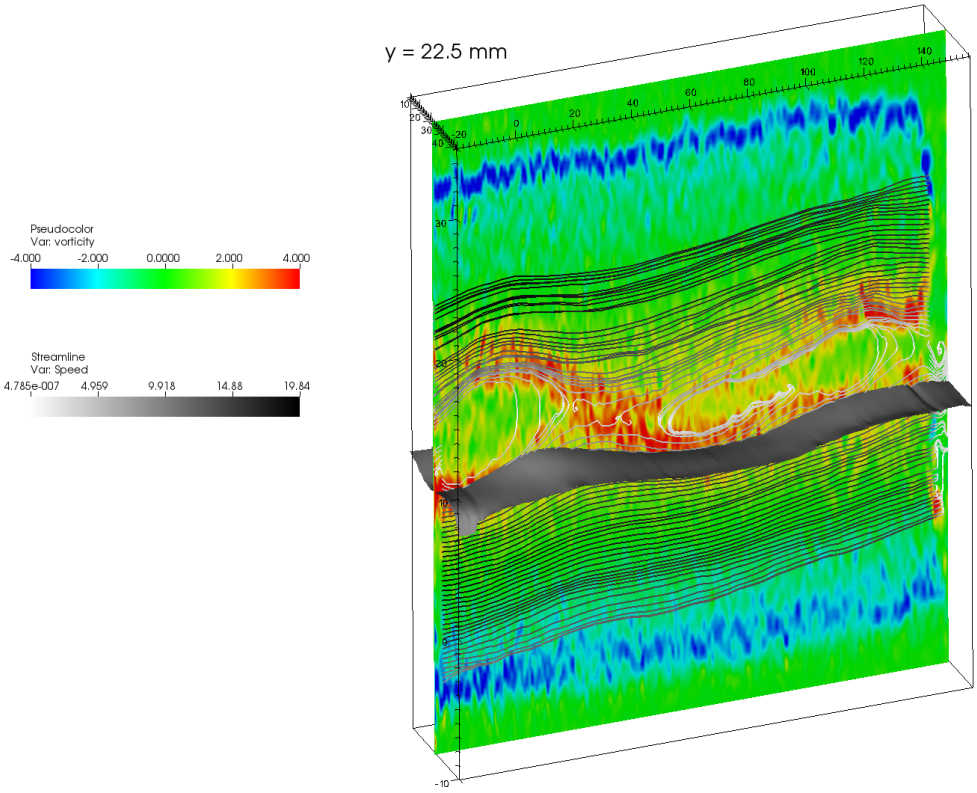

Figure 5: Data of figure 4a, superimposed with cross-plane vorticity (z axis is stretched by a factor of 5).

The Holmboe waves, first reported in Holmboe (1962) typically feature a succession of upward and downward pointing cusps, travelling on the interface in opposite directions. They result from the saturation of the Holmboe instability, a stratified shear instability often observed when the density interface is much thinner than the shear layer. The instability can be seen from a wave-interaction perspective as the interaction of three waves: one gravity wave at the sharp density interface, and two Rayleigh waves, one at each vorticity gradient interface, sandwiching the gravity wave. This interaction gives rise to two distinct growing modes with opposite phase speeds and cusps pointing in opposite directions due to vortices sandwiching the density interface. The snapshot of figure 4 focuses on the spatial structure of such a wave, of which we observe slightly more than one wavelength, with $\lambda \approx 100$ mm. Two other interesting features deserve our attention. First, the wave amplitude is larger in the middle of the channel, being maximum in the mid-plane $y = 22.5$ mm, presumably due to the influence of the side-walls. Second, focusing on the 2D streamlines around the interface plotted in the mid-plane in figure 4a-b, we see that vortices are indeed observed at the top of both upward cusps (where the flow should be right to left sufficiently far above), indicating recirculation. Why such structures are not observed below the density interface is still unclear however. In figure 4c, a slice in a slightly off-centred plane $y = 28$ mm shows some variations that hint at the 3D structure of those vortices. The structure of the vorticity shown in figure 5, composed of long filaments of high vorticity around the interface, has been consistently observed in the Holmboe regime. They were present in §1, figure 2 top right panel, and it is tempting to correlate their progressive breakdown into two series of filamented structures (middle right panel) featuring increase disorder (bottom right) with the onset of turbulence.

Finally, a slightly different wave regime can be observed for the same flow parameters as previously, but when the experiment is started with a thicker density interface (figure 6). This was achieved in this example by adding the salts to each reservoir after closing

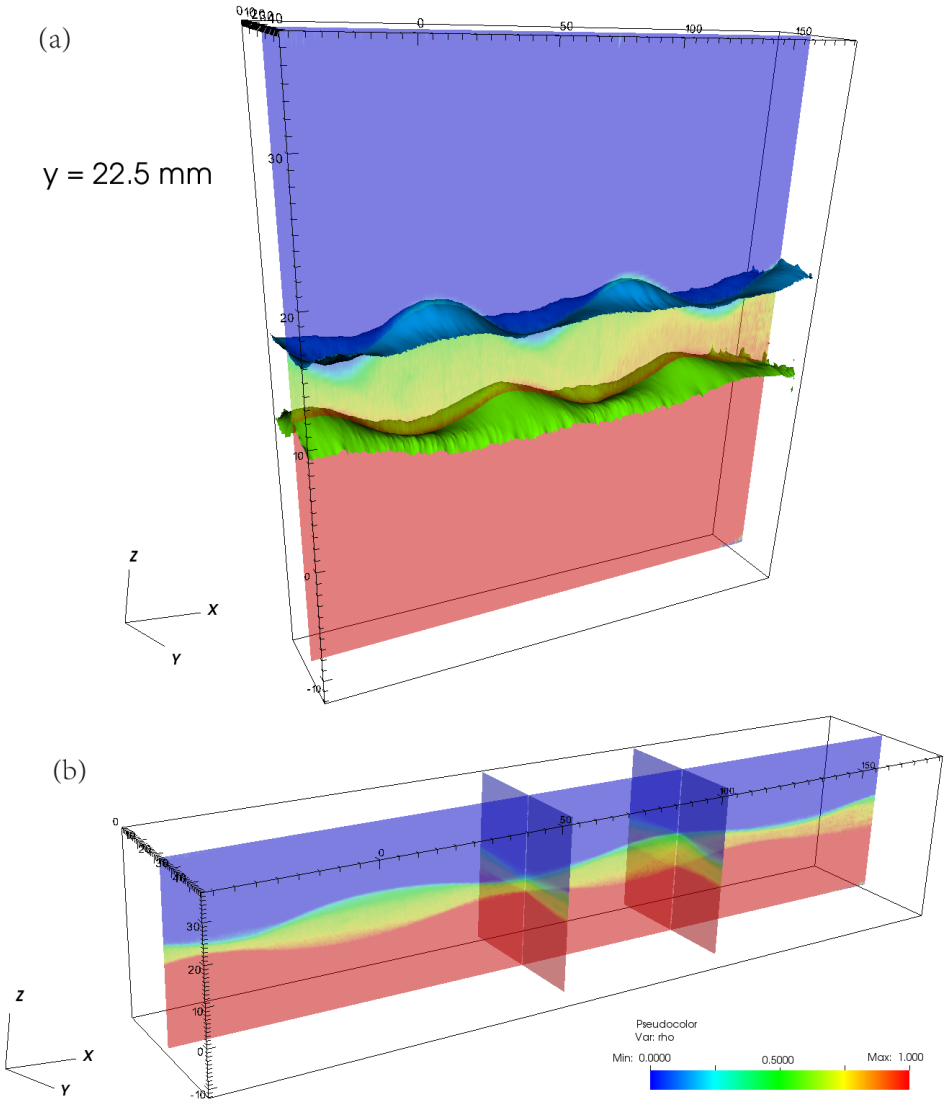

Figure 6: (a) Two isodensity surfaces, with the $y = 22.5$ mm density field (z axis stretched by 5). (b) A a slightly different time: (x, z) density field as in (a), with additional (y, z) slices (to scale).

the duct ends, such that the duct contained fresh water initially. Opening the ducts at the start of the experiment resulted in the development of two turbulent gravity currents in fresh water (as opposed to a laminar one, previously, between the salt solutions when the duct initially contained one of the solution). The turbulence decays quickly but the mixed fluid generated by this initial event remains at the interface, due to the very slow velocity there. The resulting three-layer flow is visualised in figure 6a-b by various planes of the density field as well as with two superimposed isodensity surfaces in figure 6a. The presence of two distinct spatial structures on each side of the interface is apparent, and the temporal data shows that, contrary to the previously described Holmboe waves, these are almost stationary, their phase speed being only of order 1% of the flow velocity (≈ 0.2

mm.s^{-1}). Figure 6a-b are taken at slightly different times and show the top and bottom waves with slightly different phase shifts. The 3D structure of the isosurfaces is however reminiscent of the one observed previously.

4 Summary and future directions

In this paper we have argued that the inclined duct experiment provides very good conditions for the study of stratified turbulence, that is, the regime in which buoyancy and turbulence are both significant. We showed in §1 that this experiment hosts qualitatively distinct flow regimes, in particular laminar wave propagation and breakdown to turbulence, and it is believed that high levels of turbulent dissipation can be controlled by the inclination angle for extended periods of time. In §2 we have presented a new experimental setup relying on a traversing laser sheet which enables quasi-instantaneous 3D velocity and density measurements in a volume of the duct. Such measurements have been applied in §3 first to visualise Holmboe waves in 3D, and then to a slightly different flow featuring two quasi-steady waves on both sides of a mixed layer.

The specifications given in §2 can be amended to probe the faster and more challenging flows characteristic of turbulence, and this is the focus of current and future efforts. We believe those new measurement capabilities are a step towards a quantitative experimental study of the stratified turbulent regime and its mixing characteristics.

References

Bartello, P. and Tobias, S. M. (2013). Sensitivity of stratified turbulence to the buoyancy Reynolds number. *Journal of Fluid Mechanics*, 725:1–22.

Holmboe, J. (1962). On the behaviour of symmetric waves in stratified shear layers. *Geofys. Pub.*, 24:67–112.

Kiel, D. E. (1991). *Buoyancy driven counterflow and interfacial mixing.* PhD thesis, University of Cambridge.

Macagno, E. O. and Rouse, H. (1961). Interfacial mixing in stratified flow. *Journal of the Engineering Mechanics Division. Proceeding of the American Society of Civil Engineers*, 87(EM5):55–81.

Meyer, C. R. and Linden, P. F. (2014). Stratified shear flow: experiments in an inclined duct. *Journal of Fluid Mechanics*, 753:242–253.

Waite, M. L. (2014). Direct numerical simulations of laboratory-scale stratified turbulence. *Modelling Atmospheric and Oceanic Flows: Insights from Laboratory Experiments (ed. T. von Larcher & P. Williams), American Geophysical Union.*